Study of titanium alloy Ti–Al–Zr–Nb–V during heating under deformation and its phase transformation features

Aidar KENZHEGULOV[1,*] Axaule MAMAEVA[1], Aleksander PANICHKIN[1], Akerke IMBAROVA[1],
Balzhan KSHIBEKOVA[1], Rashida AUBAKIROVA[1], Natasha SATKANOVA[2], and Nazgul TOIYNBAEVA[3]

[1] *JSC "Institute of Metallurgy and Ore Beneficiation", Almaty, Republic of Kazakhstan*

[2] *Satbayev University, Almaty, Republic of Kazakhstan*

[3] *Almaty Technological University, Almaty, Republic of Kazakhstan*

*Corresponding author e-mail: a.kenzhegulov@satbayev.university

Abstract

An alloy based on Ti–Al–Zr–Nb–V was prepared and its deformation behavior at elevated temperatures was studied. The microstructure and phase of the alloys were characterized by optical microscopy, scanning electron microscopy, thermal analysis, and mechanical testing. The results showed that the Ti–Al–Zr–Nb–V alloy, when stretched, exhibits a superplasticity effect in the range of 975°C to 1100°C, with an elongation of up to 400%. It was found that superplasticity develops in the temperature region of the α+β→β transition and is accompanied by a change in grain size and redistribution of alloying elements among phases.

1. Introduction

Today, titanium and its alloys have received much attention and are used in many fields due to their good biocompatibility, high strength-to-weight ratio, excellent wear and corrosion resistance, acceptable creep, and fatigue properties [1-4]. One of the interesting properties of titanium alloys is superplasticity [5,6]. The use of the superplasticity effect makes it possible to significantly reduce deformation forces compared to traditional methods of hot metal forming and isothermal deformation, and to use low-power equipment. Superplastic deformation processes are promising for the manufacture of workpieces of complex shapes, they can significantly increase the utilization rate of metals and their durability, reduce the energy intensity and cost of technological processes, and the consumption of expensive materials [7-9].

The formability of titanium alloys is enhanced by decreasing grain size [10], high temperatures [11], and low strain rates [12]. Unfortunately, this makes the processing and production of components expensive and inefficient [13]. Consequently, although the mechanisms of superplastic deformation in titanium alloys are well known [14,15], there is still a search for new solutions, which are mainly aimed at optimizing the microstructure and the balance between the shares of the α/β phase. In initiating superplasticity, the most important factor is the preliminary preparation of the fine-grained structure of the alloys or its transfer to another metastable state.

Li S. *et al.* reported that major α martensite and minor β martensite are formed in Ti–20Zr–8Nb–3Sn sample. When the Nb content increases above 10 at%, only the β phase is observed [16]. Fu J. *et al.* [17] developed a Ti-18Zr-4.5 Nb-3Sn-2Mo alloy by replacing Nb with Mo and confirmed that this increases the tensile strength, thereby increasing the critical stress. Superelasticity due to the introduction of Cr into the alloy of a wrought Ti-Zr-Nb-Sn alloy was confirmed by the authors of [18]. As the above and other works [19,20] show in this area, theoretical and experimental research into the causes of unusually high deformability of the material and the mechanisms of superplastic deformation is of great interest. However, according to our data, superplasticity, and phase transformation of the Ti–Al–Zr–Nb–V alloy have not yet been studied. For this reason, we focused on the results of the microstructure and thermal analysis of titanium alloy Ti–Al–Zr–Nb–V. The purpose of the work is to study the titanium alloy Ti–Al–Zr–Nb–V (alloy grade 27) when heated for deformation.

2. Experimental

In our work, we studied titanium pseudo α - alloy grade 27, containing Ti + (3.0 to 4.2)% Al + (0.7 to 1.5)% Nb + (0.7 to 1.5)% V + (2.0 to 3.0)% Zr. By using various types of thermal and thermo-mechanical processing - hot forging, annealing, quenching, and tempering, the alloys were brought into the following states:

1) initial - the state of forgings annealed in the range (α+β), then cooled in air,

2) hot-forged rods, heat-treated to fine grain (annealing at 800℃ for 1 h, quenching in water),

3) heat-treated for large grains (annealing of forged rods at 1150℃ for 30 min, cooling in air).

Thermal analysis was carried out using a simultaneous thermal analysis instrument STA 449 F3 Jupiter (Netzsch, Germany). The samples were heated at rates of 20℃·min^{-1}, 15℃·min^{-1}, 10℃·min^{-1}, 5℃·min^{-1}, in an atmosphere of highly purified argon up to 1100℃. Cooling was carried out to 500℃ to 400℃ at rates exceeding the heating rate by 10℃. The results obtained with the STA 449 F3 Jupiter were processed using the NETZSCH Proteus software.

The study of the structure of sections and the distribution of elements in the alloy was carried out using scanning electron microscopy on a Jeol – JXA8230 microprobe (Jeol, Japan) by wave dispersion analysis and scanning electron dispersion analysis at a beam current of 5 nA and an accelerating voltage of 20 kV.

Detailed studies of the superplastic flow of alloy 27 were carried out in the temperature range of 925℃ to 975℃ at a constant tensile rate of 1 mm·min^{-1} on a Shimadzu AG-100kN universal electro-mechanical testing machine (Shimadzu, Japan). To reduce oxidation of the sample surface during testing, argon was supplied to the furnace chamber. The machine is equipped with a high-temperature attachment with a furnace that allows testing at temperatures up to 1000℃.

3. Results and discussion

The microstructures of alloy 27 in different states differ significantly from each other (Figure 1). Hot forging is carried out first at temperatures above the (α + β) → β transition, i.e. begins in the β - region, followed by a gradual decrease and ends in the upper level of the α - region. Then the hot-heated samples have a fine-grained composition with crushed structural components. At the same time, the microstructure of the metal in large forgings reveals the beginning of the recrystallization process with the emergence of new grains against the background of martensite (Figure 1(a)), and hot forging of small rods is characterized by the crushing of martensite needles formed earlier during heating for deformation (Figure 1(b))

Titanium alloys are characterized by the formation of large polyhedral solid solution grains in the high-temperature β-region, which persist after complete cooling of the material. This feature is also observed in alloy 27; at room temperature, the framework of the b-grain boundaries is preserved (Figure 1(c)), and the inside grain structure depends on the cooling rate. With sharp cooling, acicular martensite is quenched inside the grains (Figure 1(c)), with slow cooling, the decomposition of martensite and the formation of a lamellar structure are completed. A special case of this lamellar morphology is the so-called "basket weave" structure typical of titanium alloys (Figure 1(d)).

Subsequent deformation of such rods by forging leads to a characteristic distortion of the shape of the packs of these plates; they bend and twist (Figure 1(e)). In the surface zone of a bar during hot forging, the degree of deformation is much higher than inside it. Because of this, the grains in the peripheral part are highly refined, and the high temperature leads to their recrystallization, as observed in Figure 1(f).
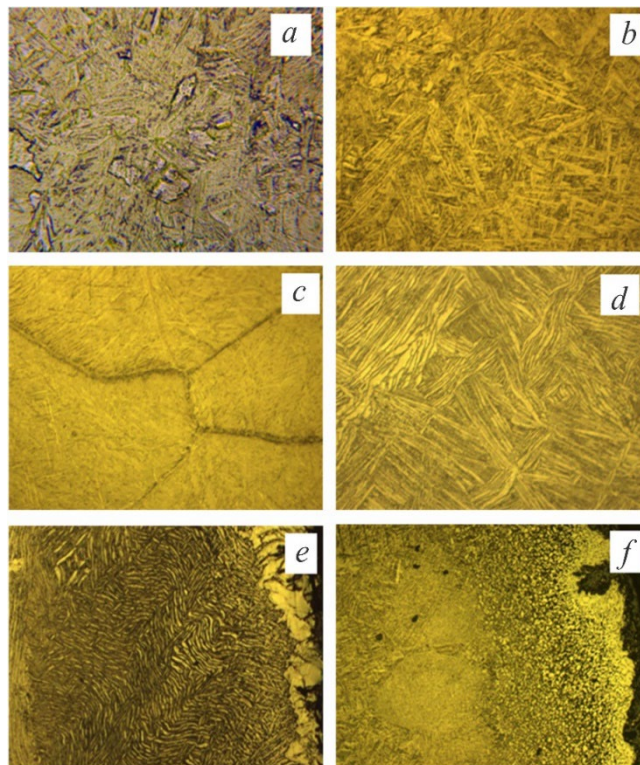
Figure 1. Microstructure of the alloy in 27 different states: (a) in the initial state of forging x500, (b) after the hot forging of rods x500, (c) annealed at 1150℃ for 30 min with rapid cooling x500, (d) annealed at 1150℃ for 30 min with slow cooling x500, (e, f) peripheral part of hot forged rod x200, x100

Thus, the microstructure of alloy 27 in annealed and then hot-forged rods is characterized by a coarse-grained structure in the volume (depending on the degree of deformation, accompanied by crushing of grains into separate blocks), and a fine-grained structure along the perimeter of the surface zone. Directly near the surface of the forged rod, a strip of an alpha layer of large light grains is formed (Figure 1(e, f)). The superplasticity of alloy 27 was studied during tensile deformation. First, traditional experiments were carried out to determine the temperature dependence of the ductility and tensile strength of the alloy with a constant speed of movement of the grips of a vertical hydraulic tensile testing machine of 4 mm·min^{-1} in the range of 600℃ to 1100℃. The samples were in the initial forging state without subsequent heat treatment, and had a heterogeneous fine microstructure of crushed martensite with signs of the beginning of recrystallization of the treatment, similar to what is seen in Fig. 1*a*.

From the halves of torn superplastic samples, both longitudinal and transverse sections were made in different sections of the sample as the degree of deformation increased. The secondary electron image (Figure 2) shows a polyhedral structure with precipitation of the second β phase at grain boundaries and at triple junctions, which confirms the two-phase nature of the material. No traces of plastic deformation are found on the microstructures; recrystallization of the processing has taken place and, in places, also collective recrystallization. The influence of deformation noticeably affects the grain size and the amount of second-phase precipitates. The higher the degree of deformation, the finer the grains and the greater the amount of β-phase precipitation. The morphology and number of phases should mainly depend on the deformation and its rate [21].
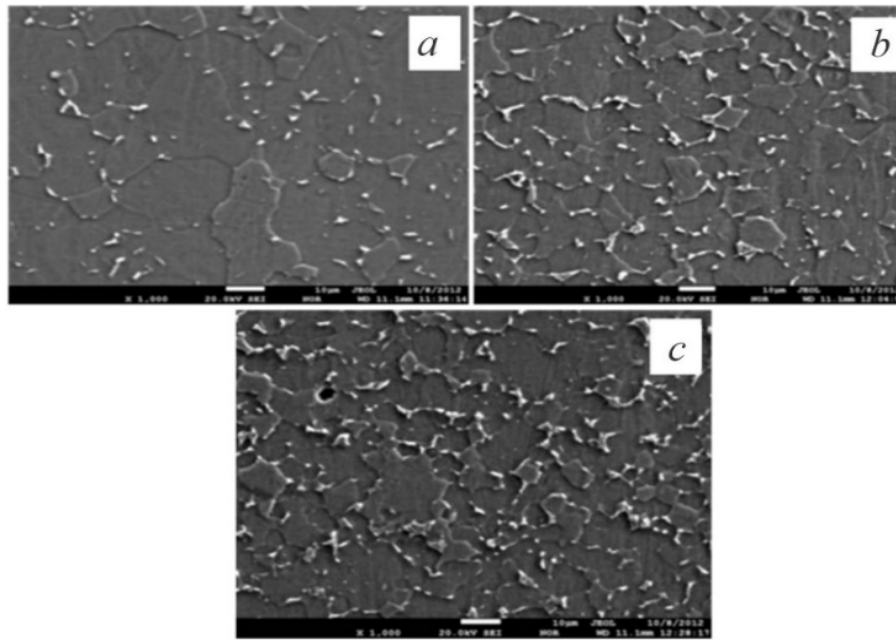
Figure 2. Image in secondary electrons of the microstructure of alloy 27 (1100°C) after plastic deformation by tension in the undeformed head of the sample (a), in the zone of medium degrees of deformation (b), and near the fracture surface (c), magnification x 1000
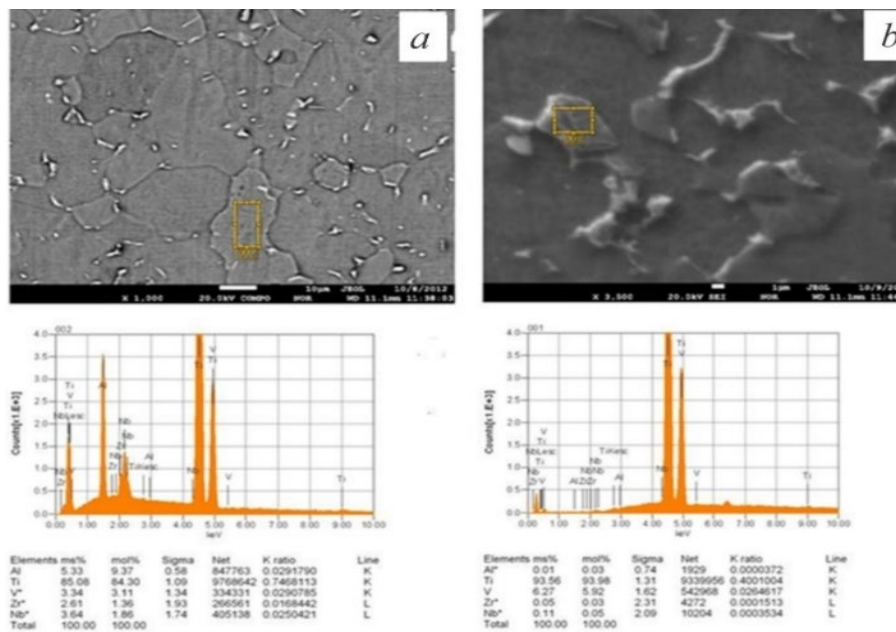
Figure 3. Energy dispersive spectrometry of characteristic X-ray radiation of a broken sample of alloy 27 in the main matrix (a), and in the second phase precipitates (b) magnification x 3500.

To identify patterns of distribution of alloying elements in the alloy, energy dispersive spectrometry of characteristic X-ray radiation was used. The results showed that the main solid solution contains about 5.33% Al and a small amount of other alloying elements, which are detected forcibly (Figure 3(a)). Wavedispersive spectrometry of a fractured sample of alloy 27 near the fracture surface is shown in Figure 4. The distribution of the main elements consists of Ti, Al, V and in the form of an overlay of the Cr line.

The second phase precipitates are solid solutions of refractory elements in titanium - vanadium, zirconium, and niobium. At the same time, in places of maximum deformation, vanadium (6.27%) is concentrated mainly in these crystals. That is, the imposition of deformation at high temperatures on titanium alloys leads to a redistribution of alloying elements (Figure 4).

Wave-dispersive spectrometry of a sample area near the rupture site also indicates that the elemental composition of the alloy underwent some changes during deformation in the direction of liberation of vanadium from the main matrix near the rupture site, while the content of aluminum, zirconium, and niobium in the titanium solid solution remained unchanged. Vanadium diffused from the grain volumes into the intergranular spaces.
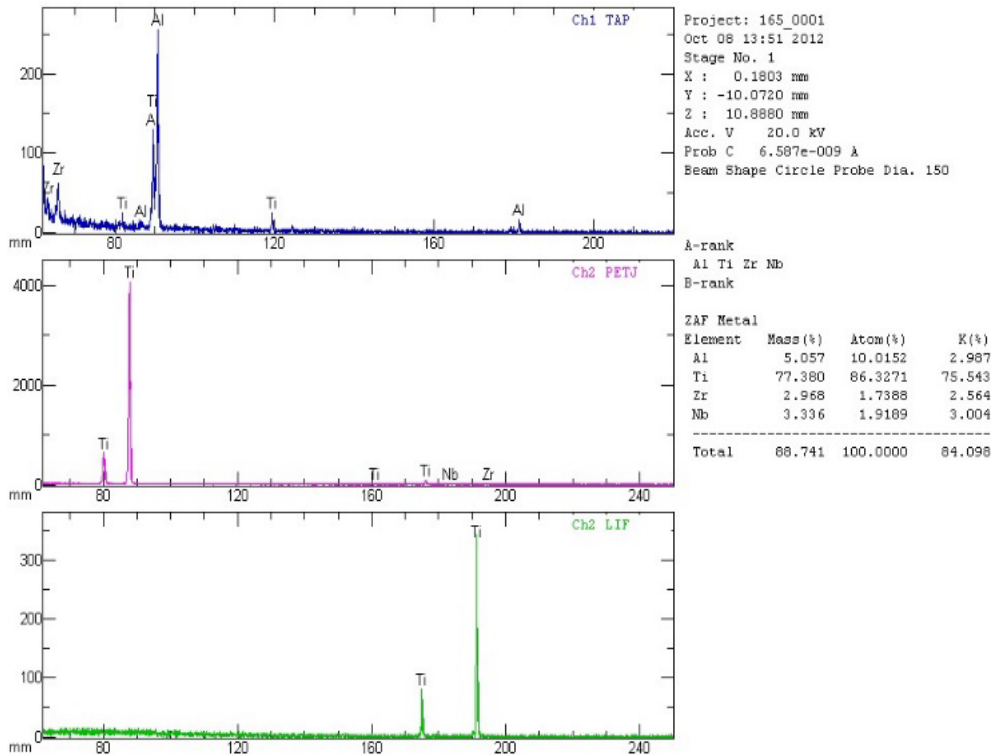
Figure 4. Wave-dispersive spectrometry of a ruptured sample of alloy 27 near the fracture surface.

(a)   **(b)**
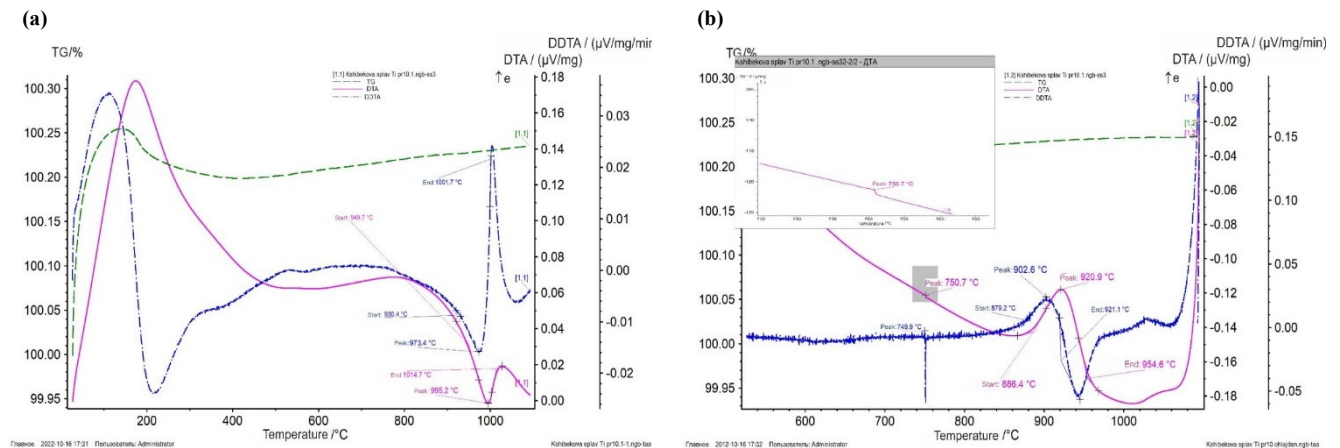
Figure 5. Results of thermal analysis of a sample of alloy 27 when heated at a rate of 20°C·min^{-1} (a), and cooled at a rate of 30°C·min^{-1} (b).

Figure 5 shows typical thermal analysis results. The DTA curve showed an endothermic effect, the onset of which occurs at 948.8°C with maximum development at 995.2°C.

The dDTA curve also showed an endothermic effect. The extreme of this effect occurred at 973.4°C. The DTA curve obtained during cooling of the sample at a rate of 30°C·min^{-1} showed an intense exothermic effect with a peak at 920.9°C and a very weak exothermic effect with a peak at 750.7°C. These effects are a reflection of phase transitions α → α + β → β. When heated, only one effect appeared on the DTA curve. A comparison of the thermal analysis data of all 14 samples showed a general pattern - the beginning of the phase transition near 940°C to 950°C, maximum development at 970°C, and completion at about 1000°C. A comparison of thermal and metallographic data leads to the conclusion that the maximum development of super-plasticity of alloy 27 is observed precisely in the temperature region of the α + β → β transition.

The ductility of alloy 27 in the temperature range of the α phase is noticeably lower than that of samples fractured above 970°C. The elongation of the sample increases with heating, forming small spikes near 700°C, 800°C, and 900°C (Figure 6).

Upon reaching the temperatures of phase transitions α → (α + β) → β, plasticity increases sharply to 170% to 180% on average, and in individual samples to 190%. In this case, the narrowing also increases to values of 0.7 to 0.9, quite sufficient to conclude that under these conditions plastic deformation with high degrees is quite possible, and the resistance to deformation sharply decreases, and the tensile strength drops to 2 kg (mm²)$^{-1}$.

Combined in Figure 7, the tensile diagrams of hot-forged samples of alloy 27 with a fine microstructure (as in Figure 1(b)) show that their maximum plasticity was observed in a fairly narrow temperature range of 937°C to 967°C. The elongation reached 400% and the samples did not undergo destruction, and the experiment was stopped due to the upper traverse of the testing machine reaching its limit position. At the initial stages of the deformation of samples, temperature significantly affects the stresses arising in them, while up to 967°C at identical degrees of deformation, stresses naturally decrease, and above this temperature, they begin to increase. This is explained by the beginning of the appearance of the β phase in the structure of the alloy at temperatures above 967°C.

Consequently, the observed development of maximum plasticity and minimum resistance to deformation at the temperature of the phase transition is a typical effect of superplasticity transformation. Moreover, at high degrees of deformation from 240% to 400% elongation, the process of metal flow occurs at very low stresses of close magnitude, which is characteristic of "true superplasticity." A detailed analysis of the stress-strain diagrams and the shape of the fractured samples after cooling confirms this conclusion. Figure 8 shows numerous areas of deformation localization at large degrees of deformation of the sample, that is, the development of a quasi-uniform flow with the so-called "running neck" took place.
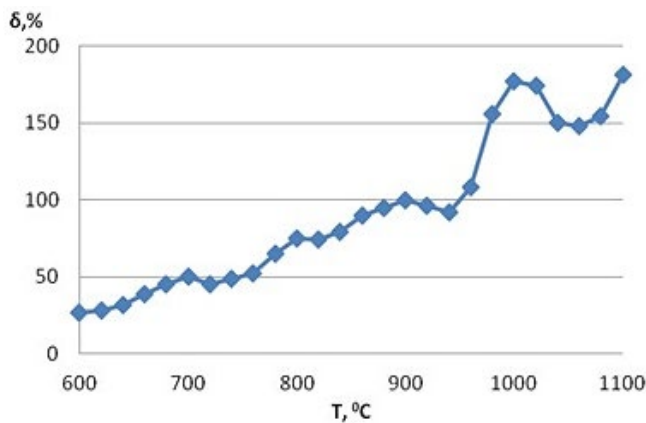
Figure 6. Temperature dependence of elongation of alloy 27 at rupture at a speed of 4 mm·min^{-1}
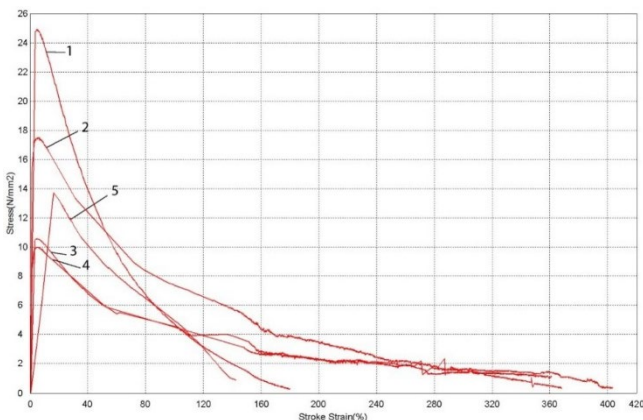
Figure 7. Strain diagrams of alloy 27 at a strain rate of 1 mm·min^{-1} and various temperatures:`1 – 925°C, 2 – 937°C, 3 – 950°C, 4 – 967°C, 5 – 975°C
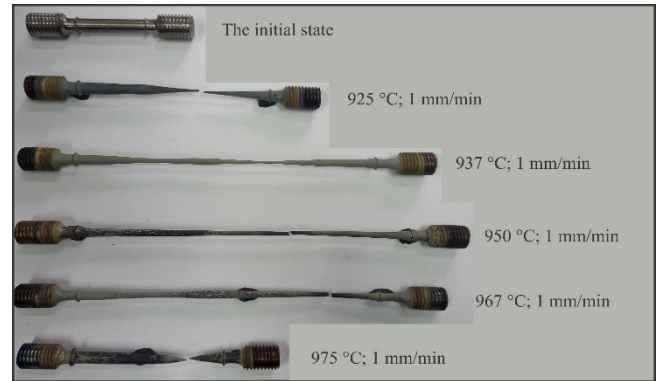
Figure 8. Shape of alloy 27 samples at a strain rate of 1 mm·min^{-1}

4. Conclusions

Thus, alloy 27, when stretched, exhibits the effect of superplasticity in the range of 975°C to 1100°C, with elongation up to 400% being a typical manifestation of superplasticity transformation. It develops in the temperature region of the α + β → β transition and is accompanied by a change in grain size and redistribution of alloying elements among phases. The elongation in case of rupture of samples in the range of 925°C to 975°C at a constant stretching rate of 1 mm·min^{-1} is 400%.

Acknowledgements

References

[1]. L. Sheng, Y. Yang, C. Lai, X. Chen, and T. Xi, "Microstructure evolution of a Ti–Al–Sn–Zr based alloy during the hot compression deformation," *Materials express*, vol. 9, pp. 1127-1133, 2019.

[2]. M. Jayaprakash, D. H. Ping, and Y. Yamabe-Mitarai, "Effect of Zr and Si addition on high temperature mechanical properties of near-Ti–Al–Zr–Sn based alloys," Materials Science & Engineering A, vol. 612, pp. 456-461, 2014.

[3]. A. Mamaeva, A. Kenzhegulov, P. Kowalewski, and W. Wieleba, "Investigation of hydroxyapatite-titanium composite properties during heat treatment," *Acta of Bioengineering and Biomechanics*, vol. 19, no. 4, pp. 161-169, 2017.

[4]. M. A. Alipovna, K. A. Karaulovich, P. A. Vladimirovich, A. Z. Zhanuzakovich, B. Kshibekova, W. Wieleba, T. Lesniewski, and N. Bakhytuly, "The study of the tribological properties under high contact pressure conditions of TiN, TiC and TiCN coatings deposited by the magnetron sputtering method on the AISI 304 stainless steel substrate," *Materials Science- Poland*, vol. 41, no. 1, pp. 1-14, 2023.

[5]. S. L. Semiatin, V. Seetharaman, and I. Weiss, "Hot workability of titanium and titanium aluminide alloys-an overview,"

Materials Science & Engineering A, vol. 243, no. 1-2, pp. 1-24, 1998.

[6]. E. Alabort, D. Putman, and R. C. Reed, "Superplasticity in Ti–6Al–4V: Characterisation modelling and applications," *Acta Materialia*, vol. 95, pp. 428-442, 2015.

[7]. A. V. Sergueeva, V. V. Stolyarov, R. Z. Valiev, and A. K. Mukherjee, "Advanced mechanical properties of pure titanium with ultrafine grained structure," *Scripta Materialia*, vol. 45, pp. 747-752, 2001.

[8]. V. F. Korshak, and Yu. A. Shapovalov, "Some aspects of superplastic flow of eutectic alloys related to metastability," *Physics of metals and metallurgist*, vol. 107, no. 4, pp. 422-428, 2009. (Rus)

[9]. V. P. Poida, V. V. Bryukhovetskii, A. V. Poida, R. I. Kuznetsova, V. F. Klepikov, and D. L. Voronov, "Morphology and mechanisms of the formation of fiber structures upon high-temperature superplastic deformation of aluminum alloys," *The Physics of Metals and Metallography A*, vol. 103, no. 4, pp. 414-423, 2007.

[10]. A. E. Geckinli, "Grain boundary sliding model for superplastic deformation," *Metal science*, vol. 17, no. 1, pp. 12-18, 1983.

[11]. T. G. Langdon, "Seventy-five years of superplasticity: historic developments and new opportunities," Journal of materials science, vol. 44, no. 22, pp. 5998-6010, 2009.

[12]. S. Roy, and S. Suwas, "The influence of temperature and strain rate on the deformation response and microstructural evolution during hot compression of a titanium alloy Ti–6Al–4V–0.1 B," *Journal of Alloys and Compounds*, vol. 548, pp. 110-125, 2013.

[13]. E. Alabort, D. Barba, M. R. Shagiev, M. A. Murzinova, R. M. Galeyev, O. R. Valiakhmetov, A. F. Aletdinov, and R. C. Reed, "Alloys-by-design: application to titanium alloys for optimal superplasticity," *Acta Materialia*, vol. 178, pp. 275-287, 2019.

[14]. Q. Bai, J. G. Lin, T. A. Dean, D. S. Balint, T. Gao, and Z. Zhang, "Modelling of dominant softening mechanisms for Ti-6Al-4V in steady state hot forming conditions," *Materials Science and Engineering A*, vol. 559, pp. 352-358, 2013.

[15]. Q. J. Sun, G. C. Wang, and M. Q. Li, "The superplasticity and microstructure evolution of TC11 titanium alloy," *Materials & Design*, vol. 32, no. 7, pp. 3893-3899, 2011.

[16]. S. Li, J. H. Lim, I. U. Rehman, W. T. Lee, J. G. Kim, J. S. Oh, T. Lee, and T. H. Nam, "Tuning the texture characteristics and superelastic behaviors of Ti–Zr–Nb–Sn shape memory alloys by varying Nb content," *Materials Science and Engineering A*, vol. 845, pp. 143243, 2022.

[17]. J. Fu, H. Y. Kim, and S. Miyazaki, "Effect of annealing temperature on microstructure and superelastic properties of a Ti-18Zr-4.5 Nb-3Sn-2Mo alloy," *Journal of the mechanical behavior of biomedical materials*, vol. 65, pp. 716-723, 2017.

[18]. L. Kong, B. Wang, X. Meng, and Z. Gao, "Superelasticity by introductions of Cr into the Ti-Zr-Nb-Sn strain glass alloy toward the elastocaloric application, " *Journal of Alloys and Compounds*, vol. 935, pp. 168156, 2023.

[19]. R. Kapoor, J. K. Chakravartty, C. C. Gupta, and S. L. Wadekar, "Characterization of superplastic behaviour in the (α+β) phase field of Zr–2.5 wt.% Nb alloy," *Materials Science and Engineering A*, vol. 392, no. 1-2, pp. 191-202, 2005.

[20]. W. D. Zhang, Z. Wu, Y. Liu, H. Bei, B. Liu, and J. Qiu, "Plastic deformation mechanism of Ti–Nb–Ta–Zr–O alloy at cryogenic temperatures," *Materials Science and Engineering A*, vol. 765, pp. 138293, 2019.

[21]. W. Wang, X. Zhang, and J. Sun, "Phase stability and tensile behavior of metastable Ti–V–Fe and Ti–V–Fe–Al alloys," *Materials Characterization*, vol. 142, pp. 398-405, 2018.